AD_____

AWARD NUMBER: **W81XWH-12-1-0282**

TITLE: **Monoamine Oxidase A: A Novel Target for Progression and Metastasis of Prostate Cancer**

PRINCIPAL INVESTIGATOR: **Jean C. Shih, PhD**

CONTRACTING ORGANIZATION: University of Southern California
Los Angeles, CA 90089-0001

REPORT DATE: **October 2014**

TYPE OF REPORT: **Annual Report**

PREPARED FOR: **U.S. Army Medical Research and Materiel Command**
Fort Detrick, Maryland 21702-5012

REPORT DOCUMENTATION PAGE

Form Approved
OMB No. 0704-0188

1. REPORT DATE	2. REPORT TYPE	3. DATES COVERED
October 2014	Annual	30 Sep 2013 – 29 Sep 2014

4. TITLE AND SUBTITLE
Monoamine Oxidase A: A Novel Target for Progression and Metastasis of Prostate Cancer

5a. CONTRACT NUMBER

5b. GRANT NUMBER
W81XWH-12-1-0282

5c. PROGRAM ELEMENT NUMBER

6. AUTHOR(S)
Dr. Jean C. Shih
Dr. Bogdan Z. Olenyuk

E-Mail: jcshih@usc.edu and bogdan@usc.edu

5d. PROJECT NUMBER

5e. TASK NUMBER

5f. WORK UNIT NUMBER

7. PERFORMING ORGANIZATION NAME(S) AND ADDRESS(ES)
University of Southern California
Los Angeles, CA 90089-0001

8. PERFORMING ORGANIZATION REPORT NUMBER

9. SPONSORING / MONITORING AGENCY NAME(S) AND ADDRESS(ES)
U.S. Army Medical Research and Materiel Command
Fort Detrick, Maryland 21702-5012

10. SPONSOR/MONITOR'S ACRONYM(S)

11. SPONSOR/MONITOR'S REPORT NUMBER(S)

12. DISTRIBUTION / AVAILABILITY STATEMENT
Approved for Public Release; Distribution Unlimited

13. SUPPLEMENTARY NOTES

14. ABSTRACT

The purpose of this project is to investigate the key roles of the monoamine oxidase A (MAOA) enzyme in the progression and metastasis of prostate cancer (PCa). Throughout the Year 2 of this grant we focused our effort on studying the functional and mechanistic roles of MAOA in promoting tumor metastasis to bone. We showed that genetic silencing of MAOA in C4-2 and ARCaP$_M$ human PCa lines markedly reduced tumor-invading bone lesions. We also investigated the molecular mechanisms underlying the MAOA functions in PCa by defining its roles in converging reactive oxygen species production and augmentation of HIF1α-mediated signaling. We developed a scalable synthesis of MHI-clorgyline, a novel pharmacological inhibitor of MAOA, which by inhibition of MAOA activity resulted in reduction in expression of oncogenes and cell cycle regulators that promote EMT and cancer cell invasion and migration, suggesting anti-proliferative and anti-metastatic activity of the conjugate.

15. SUBJECT TERMS
Nothing Listed

16. SECURITY CLASSIFICATION OF:			17. LIMITATION OF ABSTRACT	18. NUMBER OF PAGES	19a. NAME OF RESPONSIBLE PERSON
a. REPORT	b. ABSTRACT	c. THIS PAGE			USAMRMC
U	U	U	UU	19	19b. TELEPHONE NUMBER *(include area code)*

Table of Contents

1. **INTRODUCTION: Monoamine Oxidase A (MAOA)**, the subject of the present study, is a mitochondria-bound enzyme that oxidatively deaminates monoamine neurotransmitters and dietary amines and produces hydrogen peroxide, a major source of reactive oxygen species (ROS).(*1, 2*) ROS causes DNA damage and tumor initiation.(*3-5*) **The purpose of this research** is 1) to seek fundamental mechanistic insights on the functional roles of MAOA in human prostate cancer (PCa) progression and metastasis, and 2) to design and develop novel and effective tumor-specific pharmacological inhibitor of MAOA and to determine its effect on PCa tumor growth and metastasis in tumor xenograft mouse models. **The scope of this research** involves experiments and assays to study the role of MAOA in PCa progression and metastasis *in vitro* [LNCaP (androgen-sensitive) and C4-2B (derived from LNCaP, androgen-insensitive) and PC-3 (androgen-insensitive) PCa cells] and in mice [tumor growth studies, and tumor metastasis to bone and soft tissues]. (*6, 7*)

2. **KEYWORDS:** Prostate cancer (PCa), monoamine oxidase A (MAOA), MHI-clorgyline, near-infrared (NIR) emitting compound, novel target, novel therapeutic agent, HIF1α, reactive oxygen species (ROS), hydrogen peroxide (H_2O_2).

3. **OVERALL PROJECT SUMMARY:**

The objective of this study is to investigate the functional and mechanistic roles of MAOA in human PCa growth and metastasis, with the focus on epithelial-to-mesenchymal transition (EMT), reactive oxygen species (ROS), hypoxia-inducible factor 1α (HIF1α) and biomarkers associated with PCa progression. Furthermore, we designed, synthesized and tested *in vitro* and *in vivo* a novel tumor-specific MAOA inhibitor-near infrared (NIR) dye inhibitor (NIR-MAOA inhibitor), called MHI-clorgyline, with the goal to target and image advanced and metastatic PCa in our animal models. The reported study was conducted by three collaborating labs from two organizations (the Shih lab at USC, the Zhau lab at CSMC, and the Olenyuk lab at USC). **The Shih lab** was responsible for determining MAOA effects on PCa tumor growth and metastasis in tumor xenograft mouse models and assessing the efficacy of NIR-MAOA inhibitor on tumor growth and metastasis in tumor xenograft mouse models. **The Zhau lab** was responsible for generating different genetically manipulated human PCa cell lines and assisting with extensive immunohistochemical (IHC) analysis of tumor specimens with PCa-associated biomarkers for tumor xenograft studies. **The Olenyuk lab** was responsible for chemically synthesizing and characterizing NIR-MAOA inhibitor and assisting with determination of their pharmacological effects on PCa in tumor xenograft models.

The progress during the Year 2 of this project in accordance with the detailed task assignments, as presented in SOW, is described below:

Task 1. (**Specific Aim 1A**): Determination of the effects of MAOA on human prostate tumor growth and metastasis.

1d. Prostate tumor bone metastasis studies: **intratibial injection** of PCa cells into athymic nude mice, determination of tumor growth, tumor bone metastasis status and tumor osteo-lesion post-injection by — Months 13-18

serial imaging of luc bioluminescence and X-ray, determination of tumor ROS levels at sacrifice, and IHC analysis of tumor/bone specimens post-sacrifice (cell proliferation, osteoclastic, osteoblastic, EMT and hypoxia markers).
WT and MAOA-KD luc-tagged C4-2 and $ARCaP_M$ cells will be used.
Mice will be housed at the USC animal facility.
Investigators: Haiyen Zhau (CSMC) and Jean Shih (USC)

Task 2. (**Specific Aim 1B**): Investigation of the molecular mechanisms underlying the MAOA functions in PCa by defining its roles in ROS- and HIF1α-mediated signaling.

2a. Investigation of the effect of MAOA on PHD and HIF1α activity in human PCa cells (LNCaP, C4-2 and $ARCaP_M$) and the accompanying regulation mediated by ROS generated through the MAOA action. Months 19-27
Investigator: Jean Shih (USC)

Task 3 (**Specific Aim 2**): Synthesis and characterization of novel near-infrared (NIR) dye-clorgyline conjugate, and determination of its *in vivo* inhibitory effects on tumor growth and metastasis in tumor xenograft mouse models.

3d. Determination of the *in vivo* effect of NIR-clorgyline on prostate tumor metastasis: **intracardiac injection** of PCa cells into athymic nude mice, assessment of NIR-clorgyline targeting of metastatic tumors by superimposing both images of luc bioluminescence and NIR fluorescence, determination of tumor metastasis status and osteo-lesion post-injection of NIR-clorgyline by serial imaging and X-ray, and IHC analysis of tumor/bone specimen post-sacrifice (e.g. EMT markers) Months 13-24
Luc-tagged WT $ARCaP_M$ cells will be used.
Mice will be housed at the USC animal facility.
Investigator: Bogdan Olenyuk (USC), Haiyen Zhau (CSMC) and Jean Shih (USC)

The detailed report of our progress during this year of grant support is outlined below.

Task 1d: We performed prostate tumor bone metastasis studies through **intratibial injection** of PCa cells into athymic nude mice, and tumor growth and tumor-invading bone destruction were determined.

Human C4-2 or ARCaP$_M$ PCa cells subjected to either a scrambled control shRNA (shCon) or a *MAOA*-targeting shRNA (shMAOA) were injected intratibially into male athymic nude mice. Tumor invasion to bone was examined routinely by X-ray during the period of tumor growth (Figure 1A) and further assessed by microCT at the endpoint of experiments (Figure 1B). Serum PSA levels in mice implanted with PSA-producing C4-2 cells, which correlates to tumor growth, were collected biweekly and measured by ELISA (Figure 1C). Tumor ROS levels at sacrifice remain to be measured. Tumor specimens were fixed in formalin, embedded in paraffin, and ready for further IHC analyses of cell proliferation, osteoblastic, osteoclastic, EMT and hypoxia markers.

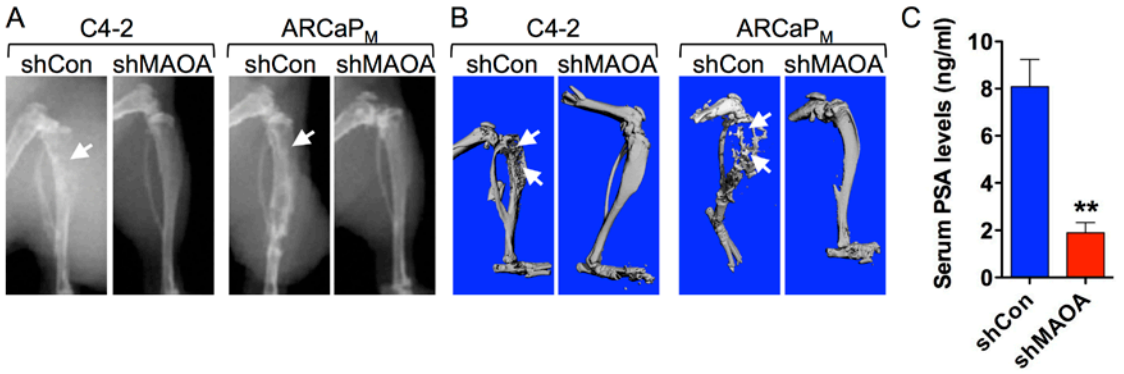

Figure 1. MAOA knockdown (KD) reduced tumor invasion to bone. **(A, B)** Representative X-ray (A) and microCT (B) images of bone destruction (week 13-19) in mice intratibially injected with scramble/MAOA-KD (shCon/shMAOA) human C4-2 or ARCaP$_M$ PCa cells. White arrows point to osteolytic lesions. **(C)** Serum prostate-specific antigen (PSA) levels that reflect intratibial C4-2 tumor growth and metastasis as measured by ELISA 6 weeks after tumor cell injection. ** p<0.01.

Conclusion: MAOA KD cells (shMAOA) have shown markedly reduced invasiveness to bone, as compared to control cells (shCon). As indicated in the Figure 1A-1B, the intratibially injected control cells produced marked bone destruction as evidenced by X-ray and microCT examination. In comparison, the bone remains essentially intact when MAOA-KD cells were used. Analysis of the serum PSA levels showed that intratibial tumor growth rate is reduced for MAOA-KD cells. This suggests that MAOA plays an essential role in promoting bone invasive properties of the PCa cells.

Task 2a: We investigated the molecular mechanisms underlying the MAOA functions in PCa by defining its roles in ROS- and HIF1α-mediated signaling. We also studied the effect of MAOA on PHD and HIF1α activity in human PCa cells (LNCaP, C4-2 and ARCaP$_M$) and the accompanying regulation mediated by ROS generated through the MAOA action.

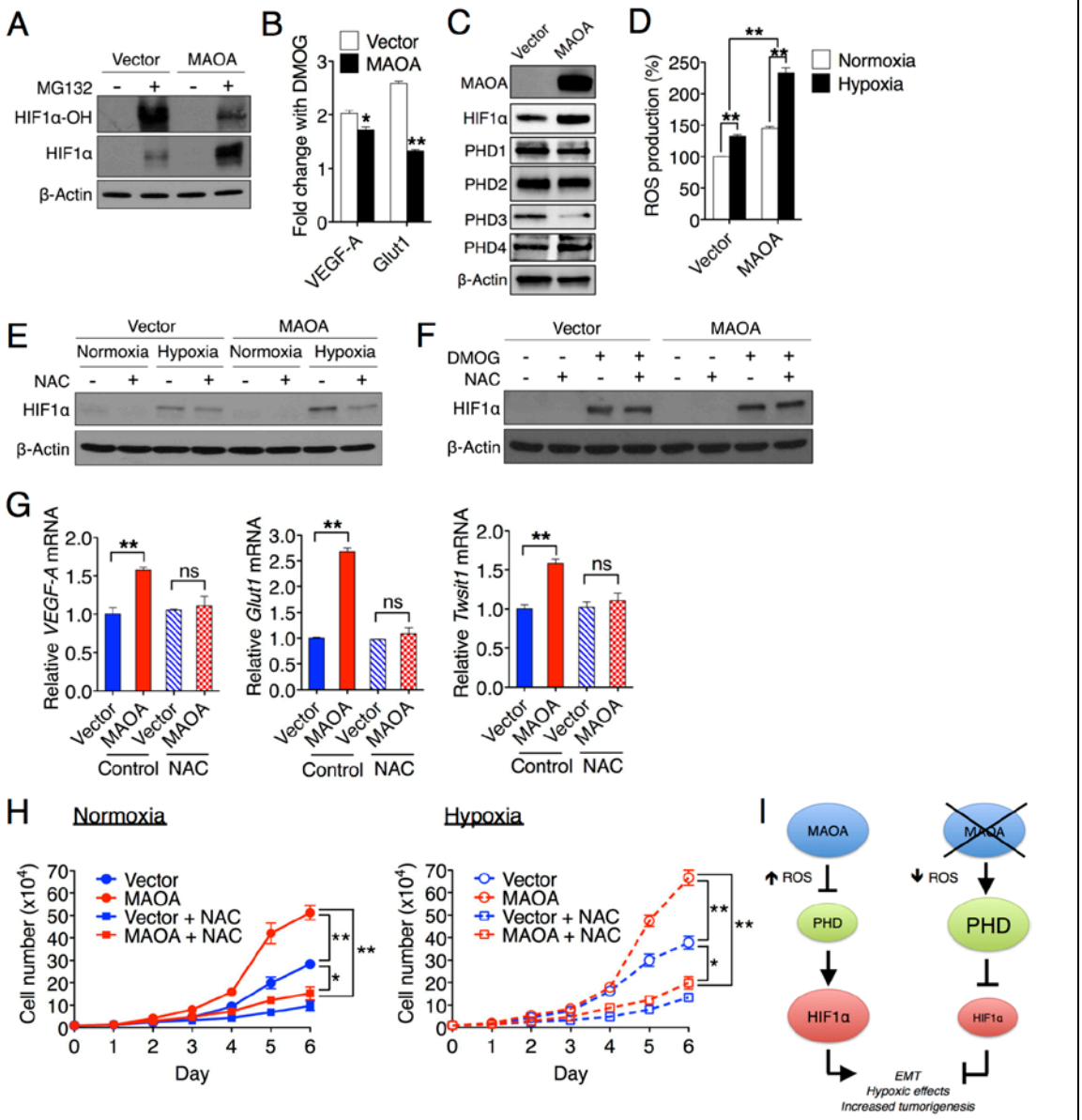

Figure 2. MAOA regulates HIF1α stability through ROS. **(A)** Immunoblots of PC-3 (vector and MAOA-ovexpression) cells treated with or without MG132 (1 μM, 6 hours) for hydroxylated HIF1α (HIF1α-OH) and total HIF1α. **(B)** Fold induction of HIF1α target genes in PC-3 (vector and MAOA-overexpression) cells treated with DMOG (1 mM, 24 hours) was measured by qPCR, and the ratio (mean ± SEM, n=3) of DMOG-treated to untreated gene expression is shown. **(C)** Immunoblots of PC-3 (vector and MAOA-overexpression) cells with hypoxia for PHD1-4. **(D)** The increase in ROS production in PC-3 (vector and MAOA-overexpression) cells with hypoxia was calculated as the percentage changes (mean ± SEM, n=3) in ROS levels in hypoxic cells relative to normoxic cells. **(E)** Immunoblots of PC-3 (vector and MAOA-overexpression) cells incubated with 10 mM NAC and cultured under normoxia and hypoxia. **(F)** Immunoblots of PC-3 (vector and MAOA-overexpression) cells cultured at 21% O_2 with 10 mM NAC or 1 mM DMOG as indicated. **(G)** qPCR analysis of *VEGF-A*, *GLUT1*, and *TWIST1* expression (mean ± SEM, n=3) in PC-3 (vector and MAOA-overexpression) cells incubated with 10 mM NAC and cultured under hypoxia. **(H)** Growth curves of PC-3 (vector and MAOA-overexpression) cells cultured in standard media supplemented with or without 10 mM NAC under either normoxia (left panel) or hypoxia (right panel) (mean ± SEM, n=3). **(I)** A schematic diagram outlining MAOA stabilization of HIF1α by repression of PHD activity through ROS production. * $p<0.05$, ** $p<0.01$.

The MAOA effect on hydroxylation-dependent HIF1α protein stability was determined by Western blot in PC-3 cells with the addition of proteasomal inhibitor (Figure 2A). The MAOA effect on PHDs enzymatic activity was examined by qPCR analysis of select HIF1α target gene expression in PC-3 cells under PHD inhibitor treatment (Figure 2B). The MAOA effect on the protein expression of all four PHD isoforms was directly measured in PC-3 cells by Western blot (Figure 2C). The interplay among MAOA-regulated HIF1α, PHD and ROS was further studied by Western blot coupled with FACS analysis of ROS levels (Figures 2D-F). The ROS effect by which MAOA mediates EMT and hypoxia was examined by qPCR analysis of select EMT and HIF1α target gene expression (Figure 2G). The role of ROS in mediating the MAOA effect on cancer cell proliferation under either normoxia or hypoxia was determined by cell number counting assays (Figure 2H).

Task 3 (**Specific Aim 2**): This Specific Aim was focused on novel clorgyline (a potent MAOA inhibitor) - near-infrared (NIR) dye conjugate (NIR-clorgyline) specifically targeting tumors. We determined the inhibitory effect of this conjugate on metastasis of human PCa in mouse models.

Task 3d-1: We studied the *in vivo* effect of NIR-clorgyline on prostate tumor growth and metastasis. We recently discovered a novel class of NIR heptamethine carbocyanine dyes, IR-783 and MHI-148, which are effective cancer-specific imaging agents. These agents show preferential uptake and retention in cancer but not normal cells. By conjugating chemotherapeutic agents with these dyes, we observed tumor-specific cell kill without cytotoxicity in host mice, suggesting the potential use of these carbocyanine dyes as carriers for cancer-specific targeting by small molecules. The advantages of this new class of dyes as imaging agents are: (I) They have relatively low molecular weights that facilitate their effective uptake into both localized and metastatic tumors; (II) They can be synthesized in pure form and are stable upon storage; (III) They are taken up by many different types of cancer cells, including circulating or disseminated tumor cells and tumor tissues regardless of their cell-surface properties and their plasticity; and (IV) They have the potential of recognizing live versus dead cells and therefore can be used for follow-up in patients subjected to treatment by hormonal, radiation and chemotherapeutic agents.

These dyes can be retained in established PCa cell lines (C4-2, PC-3 and $ARCaP_M$) with the dyes enriched in the mitochondria and lysosomes, but not in normal prostatic epithelial and fibroblast cells. In an orthotopic $ARCaP_M$ xenograft mouse model receiving intraperitoneal injection of low dose of IR-783 (10 nmol/20 g), the near-infrared signals were specifically detected in the primary tumor and its associated bone metastases within 24 hours by fluorescence optical imaging. Additionally, this novel class of dyes showed no systemic toxicity when mice were given a 100-fold excess of the imaging dose of the dye.

By using the structure-guided design we developed MHI-clorgyline, a novel tumor-targeting MAOA inhibitor that would preferentially accumulate in the PCa lesions. This inhibitor contains a tumor-targeting NIR dye and a moiety of MAOA inhibitor. We reasoned that including a NIR imaging functionality could be useful for measuring uptake and cellular localization of the conjugate and possibly for future image-guided drug delivery and diagnosis. We chose small molecule clorgyline as a MAOA-targeting functionality because of the high affinity and selectivity of this compound towards MAOA. The presence of high-resolution crystal structure

of clorgyline-MAOA complex (*8*) facilitated our design. For tumor-targeting and NIR-imaging function we chose a MHI-148 dye (*9*-*11*). The high selectivity in targeting of these dyes to tumors, mediated by tumor hypoxia and organic anion-transporting polypeptides (*12*), has been demonstrated in human PCa (*13*).

First, we developed an effective, scale-up procedure for the synthesis of MHI-clorgyline on the scale from hundreds on milligrams to 1 gram. It has been synthesized in a sequence of steps outlined in Figure 3. The synthesis started with commercially available 3-bromopropylamine hydrobromide **1**. This compound was converted into *t*-butyl (3-bromopropyl)carbamate **2**, which was used in the subsequent step to alkylate the commercially available 2,4-dichlorophenol, giving an intermediate **4**. Deprotonation of the amide in **4** was carried out with sodium hydride, followed by alkylation with propargyl bromide **5**, producing Boc-protected alkyne **6**. The protecting group was removed under acidic conditions using TFA in dichloromethane. The product **7** was alkylated with 1-bromo-3-thioacetylpropane **8**, resulting in the formation of compound **9**. Removal of the acetyl protective group in **9** was carried out in methanolic HCl, affording an intermediate **10**. This intermediate was then coupled to MHI-148 dye **11** using EDC and 4-DMAP to give MHI-clorgyline. The product was purified on preparative TLC and its identity and purity were confirmed by NMR and mass spectrometry.

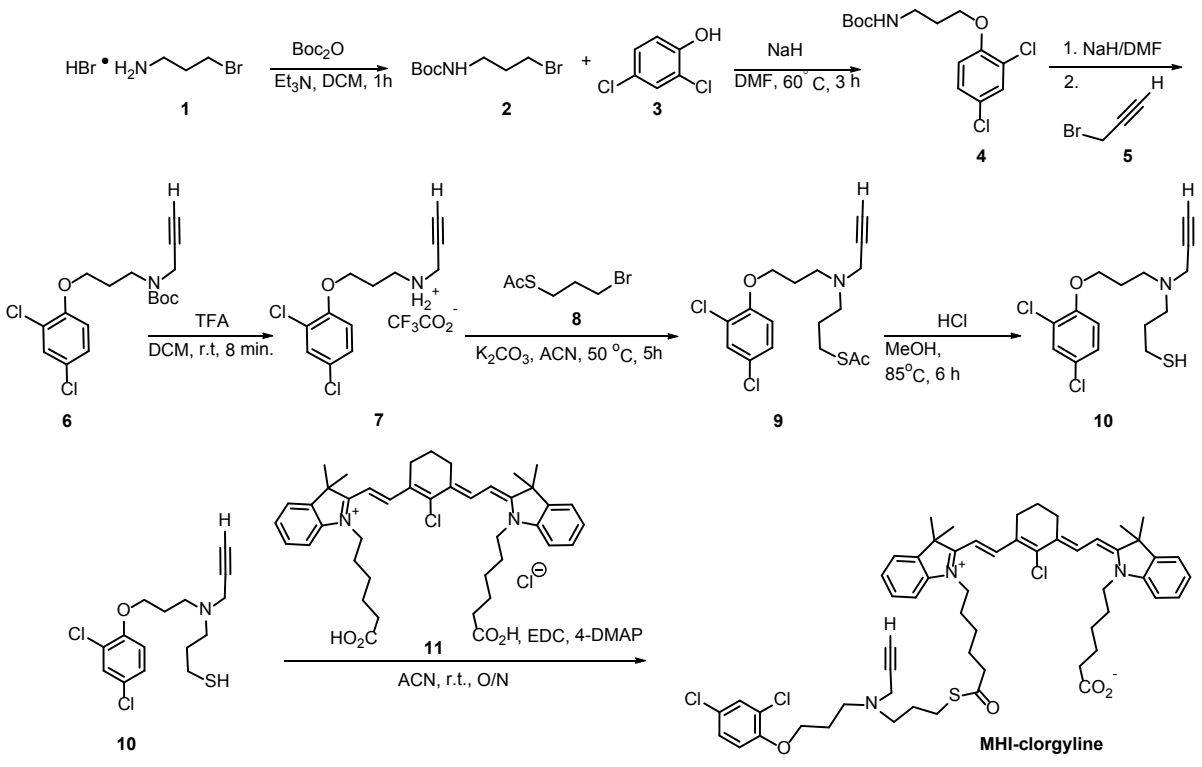

Figure 3. Scale-up synthesis of MHI-clorgyline.

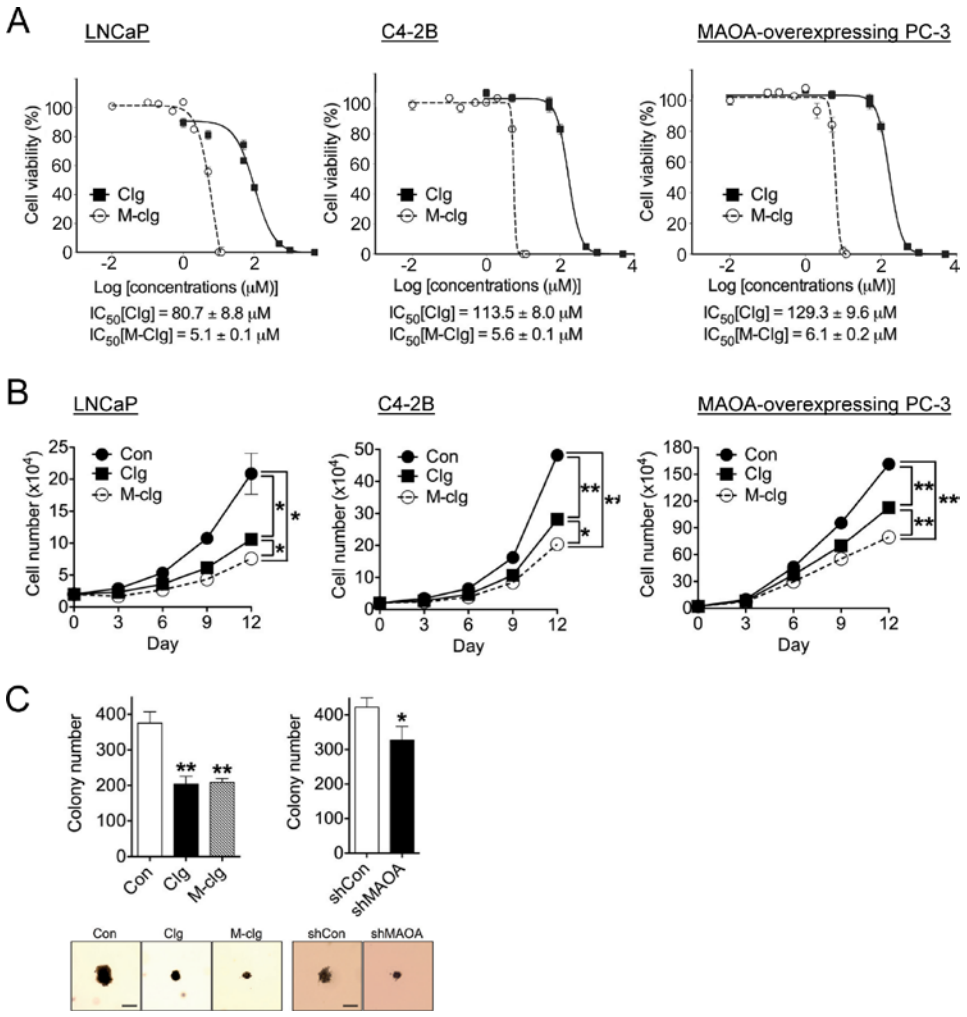

Figure 4. MHI-clorgyline inhibited PCa cell proliferation and colony formation. (A) Effect of Clg and M-clg on cell viability in LNCaP, C4-2B and MAOA-overexpressing PC-3 cells as measured by MTS assays. (B) Cell number counting assays with LNCaP, C4-2B and MAOA-overexpressing PC-3 cells treated with Clg or M-clg (1 μM) for 12 days. Compound-added medium was replenished every 3 days, PBS was used as the vehicle. * $p<0.05$. (C) Colony formation assays in either LNCaP cells treated with Clg or M-clg (1 μM, left panel) or LNCaP cells targeted by either a scrambled shRNA (shCon) or a *MAOA*-targeting shRNA (shMAOA). Representative colonies are shown (left, original magnification, ×100, scale bars: 50 μm; right, original magnification, ×200, scale bars: 100 μm). * $p<0.05$, ** $p<0.01$.

We first demonstrated that MHI-clorgyline reduced colony formation, migration and invasion of PCa cells. PCa LNCaP, C4-2B and MAOA-overexpressing PC-3 cells (*14*) were used for cell viability (Figure 4A) and cell proliferation assays (Figure 4B). Treatment with clorgyline produced dose response curves with 50% inhibitory concentrations (IC_{50}) of 80.7 ± 8.8 μM in LNCaP, 113.5 ± 8.0 μM in C4-2B, and 129.3 ± 9.6 μM in MAOA-overexpressing PC-3 cells. By comparison, treatment with MHI-clorgyline produced curves with IC_{50} of 5.1 ± 0.1 μM in LNCaP, 5.6 ± 0.1 μM in C4-2B, and 6.1 ± 0.2 μM in MAOA-overexpressing PC-3 cells, indicating 12-20 times higher efficacy for MHI-clorgyline in inhibiting PCa cells growth as compared to clorgyline (Figure 2A). In cell number counting assays we observed that both

clorgyline and MHI-clorgyline reduced the number of proliferating cells after 12 days. MHI-clorgyline also showed higher efficacy as compared to clorgyline (Figure 4B).

Colony formation assays were performed in LNCaP cells treated with clorgyline or MHI-clorgyline (Figure 4C). In a parallel setup, LNCaP cells were targeted by either a *MAOA*-targeting shRNA (shMAOA) or a scrambled shRNA (shCon). Treatment with clorgyline and MHI-clorgyline resulted in a reduction of the colony number by as much as 45%, although in this assay the difference between the activities of clorgyline or MHI-clorgyline was not statistically significant (left panel). Treatment with the *MAOA*-targeting shRNA reduced colony number by only 25%, as compared to treatment with scrambled shRNA (right panel).

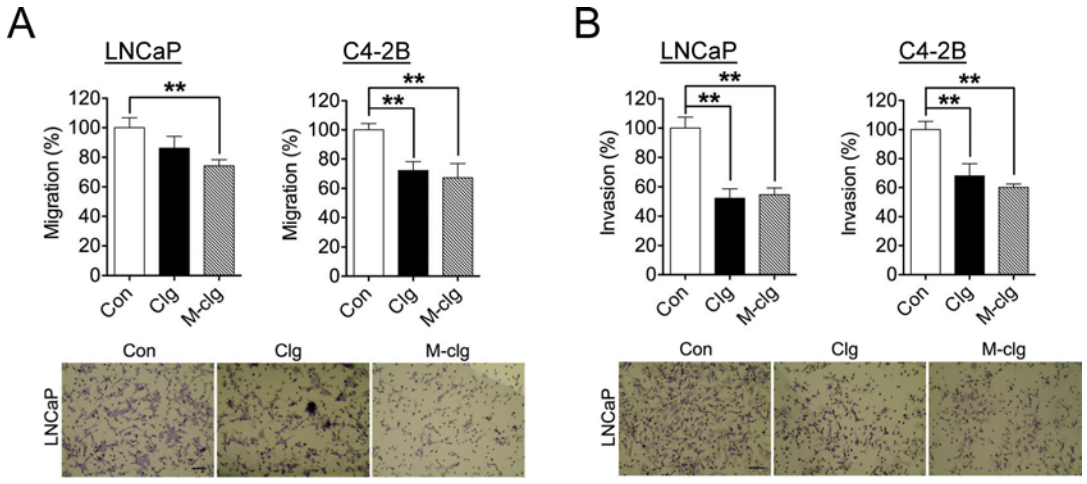

Figure 5. MHI-clorgyline reduced the migration and invasion of PCa cells.
(A) Migration assays of LNCaP and C4-2B cells treated with Clg or M-clg (1 μM, 48 hours). ** $p<0.01$. Representative images from LNCaP cells are shown. Original magnification, ×200; scale bars: 200 μm. (B) Invasion assays of LNCaP and C4-2B cells treated with clg or M-clg (1 μM, 48 hours). ** $p<0.01$. Representative images from LNCaP cells are shown. Original magnification, ×200; scale bars: 200 μm.

We determined the ability of MHI-clorgyline and clorgyline to inhibit migration of LNCaP and C4-2B cells. After treatment with compounds at 1 μM concentration for 48 hours the LNCaP cells showed statistically significant reduction in migration (20% for clorgyline, 35% for MHI-clorgyline, Figure 5A, left panel). A similar result was observed for C4-2B cells (Figure 5A, right panel). In invasion assays, cells treated with MHI-clorgyline and clorgyline also showed 50% reduction in LNCaP and 40-45% in C4-2B cells (Figure 5B).

In order to assess the efficacies of MHI-clorgyline *in vivo*, subcutaneous tumor xenograft mouse models were used. After being implanted subcutaneously into male nude mice, C4-2B cells formed tumors in 3-4 weeks. After tumors reached 200 mm^3, mice were randomly assigned into three groups to receive treatments every other day: 1) control, 2) clorgyline and 3) MHI-clorgyline. Two routes of administration were used to test the tumor-specific targeting ability of MHI-clorgyline: intratumoral and intraperitoneal. We explored an intratumoral injection because

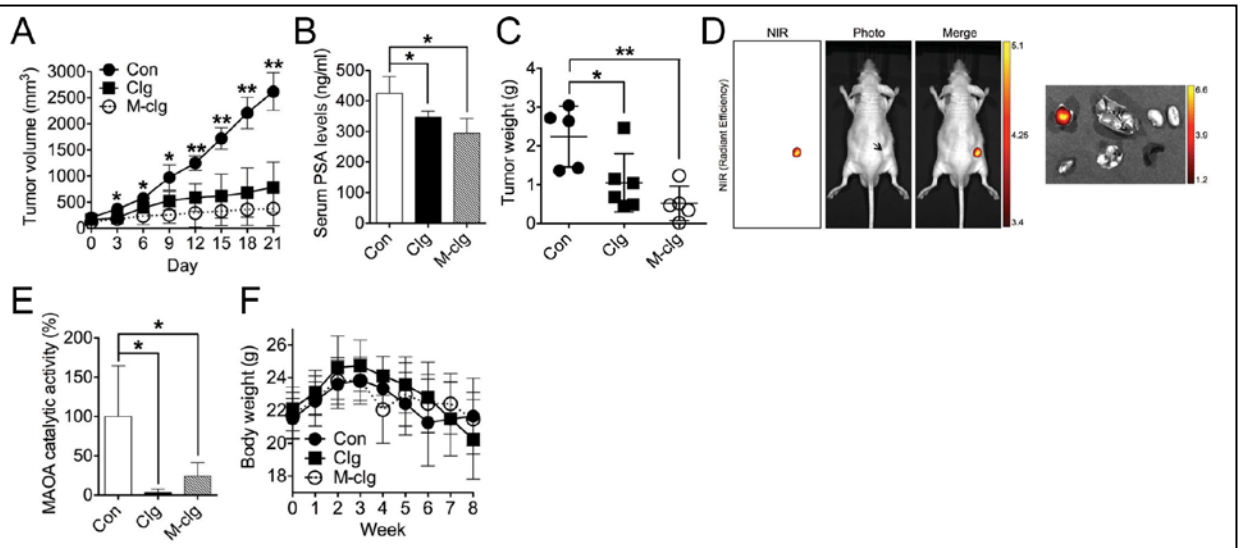

Figure 6. MHI-clorgyline inhibited the growth of C4-2B tumor xenografts in mice.
(A) C4-2B cells were subcutaneously injected into male nude mice (n=5 to 6 for each group) to establish tumor xenografts. After tumor size reached 200 mm^3, mice were given intratumoral treatments (saline, Clg; 2436 nmol/mouse and M-clg; 750 nmol/mouse) every other day for a 21-day period. Tumor size was determined by calipers and tumor volume was measured. * $p<0.05$, ** $p<0.01$. (B) Serum PSA levels in mice were determined on day 11 since the start of treatment by ELISA assay. * $p<0.05$. (C) Tumor weight was determined at the time of sacrificing mice. * $p<0.05$, ** $p<0.01$. (D) *In vivo* and *ex vivo* NIR imaging of mice given M-clg treatment. Representative images are shown. (E) Tumor MAOA catalytic activity was determined at the time of euthanasia. * $p<0.05$. (F) Mice body weight was determined every week since tumor implantation.

for clorgyline, the MAOA inhibitor without tumor-targeting specificity, this route could produce higher clorgyline concentration inside the tumor's interstitium, making more stringent conditions for comparison with the treatment efficacy of tumor-targeting MHI-clorgyline. Tumors were measured with calipers and tumor volume was calculated every three days during the 21-day treatment. Serum PSA levels in mice were determined on day 11, the middle of treatment course, and tumor MAOA activity was determined at the end of treatment. Mice body weights were monitored on a weekly basis since the time of inoculation. At the experiment endpoint mice were euthanized, tumors were excised, and tumor weights were determined. MHI-clorgyline- and clorgyline-treated mice showed significant delays in tumor growth (Figure 6A), reduction in PSA levels (Figure 6B) and decreases in tumor weight as compared to control mice (Figure 6C). It is noteworthy that even under the stringent conditions of intratumoral injection designed to improve efficacy of clorgyline, MHI-clorgyline still showed superior results. NIR imaging of the whole body *in vivo* and individual tumor and normal organs *ex vivo* clearly showed MHI-clorgyline localization within the tumor (Figure 6D). Measurements of MAOA activity in tumors showed its significant reduction in both MHI-clorgyline- and clorgyline-treated mice (Figure 4E). All mice in treated and control groups showed similar changes in body weight that did not exceed 18% throughout the entire duration of experiment (Figure 6F), suggesting that this treatment regimen was well tolerated by the animals.

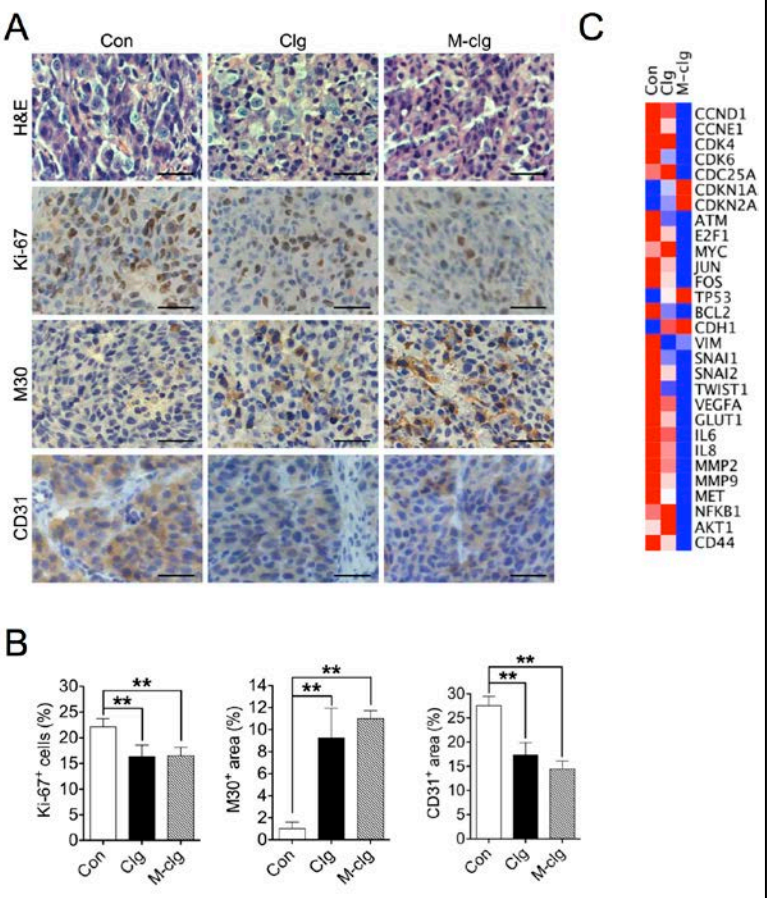

Figure 7. Analysis of tumor specimens obtained from treated and control mice.
(A) H&E and immunohistochemical analysis of Ki-67, M30 and CD31 expression in respective tumor specimens. Representative images are shown. Original magnification, ×400; scale bars: 20 μm. (B) Quantification of percent Ki-67$^+$, M30$^+$ and CD31$^+$ tumor cells or areas of five distinct images from each group. The data represent mean ± SD. ** p<0.01. (C) Heat map depicting gene expression profiling of tumor samples from each group. Red and blue colors indicate relatively high and low expression levels, respectively.

We next performed hematoxylin and eosin staining (H&E) and immunohistochemical analysis of protein expression patterns of Ki-67 (a cell proliferation marker), M30 (a cell apoptosis marker) and CD31 (an angiogenesis marker) in tumor specimens from control and treated groups (Figure 7A). H&E staining showed a decrease in the nucleus to cytoplasm ratios in cells from tumors treated by MHI-clorgyline and clorgyline, as compared to control group, suggesting reduced malignancy in treated tumors (*15*). Ki-67 staining of tumor specimens revealed a 30%–35% decrease of Ki-67$^+$ cells in MHI-clorgyline- and clorgyline-treated tumors (Figure 7B, left panel). We observed 10-12 fold increase of M30$^+$ area (middle panel) and 30-40% decrease in CD31$^+$ area (right panel) in the treated specimens as compared to controls (Figure 7B), suggesting increased apoptosis and reduced angiogenesis occurring in treated tumors. Gene expression profiling further indicated downregulation in expression of such proto-oncogenes or oncogenes as *FOS*, *JUN NFKB1* and *MYC* and upregulation of *TP53* tumor suppressor gene expression in response to treatment. Cell-cycle regulator genes that activate cell cycle progression, such as *CCND1*, *CCNE1*, *CDK4*, and *CDK6*, were also downregulated, whereas expression of select cell-cycle inhibitors, including *CDKN1A* and *CDKN2A* increased in the MHI-clorgyline- and clorgyline-treated tumors as compared to controls. In contrast, decreased expression of anti-apoptotic *BCL2* gene was revealed in treated tumor samples. In addition, genes involved in MAOA-downstream signaling demonstrated to promote EMT (*VIM*, *SNAI1*, *SNAI2* and *TWIST1*), tumor hypoxia

(*VEGFA* and *GLUT1*) and cancer cell migration, invasion and metastasis (*IL6*, *IL8*, *MMP2*, *MMP9* and *MET*) (*14*) all showed reduced expression by treatment (Figure 7C).

Conclusion: MHI-clorgyline targets tumor with no detectable accumulation in normal tissues, providing effective reduction of the tumor growth rate and tumor metastasis. Analysis of the tumor specimens shows reduction in Ki-67^+ and $CD31^+$ markers, suggesting reduction of cell proliferation and angiogenesis, and increase in $M30^+$ markers, indicating an increased apoptosis. Furthermore, gene expression profiles of tumors treated with MHI-clorgyline showed a reduction in expression of oncogenes *FOS*, *JUN*, *NFKB*, *MYC*, cell cycle regulators *CCND1*, *CCNE1*, *CDK4*/*6*, and an increase in the levels of tumor suppressor gene *TP53* and cell cycle inhibitors *CDKN1A* and *CDKN2A*. The genes downstream of MAOA, which promote EMT, tumor hypoxia and cancer cell invasion and migration, were also reduced in expression. This indicates anti-metastatic activity of MHI-clorgyline.

Task 3-2: We developed a *Pten/MAOA* double knockout (DKO) mouse model by combining prostate-specific conditional *Pten* knockout mice with *MAOA* knockout mice. We hypothesized that MAOA may act like a tumor promoter in the context of PCa through its induction of ROS and hypoxia. The resulting effect of hypoxia and ROS may result in the immune system suppression, facilitating tumor evasion from detection by the immune system. Thus, we expect that *Pten/MAOA* DKO mice would show a delayed formation of PCa tumors. This animal model will help us better understand MAOA *in vivo* functions in PCa progression and metastasis.

Conclusions: Our novel prostate-specific *Pten/MAOA* DKO mouse model will further facilitate study of the functional roles of the MAOA in prostate cancer progression and metastasis.

4. KEY RESEARCH ACCOMPLISHMENTS:

- We showed that MAOA drives tumor invasion to bone.
- We demonstrated that MAOA knockdown in both human C4-2 or $ARCaP_M$ PCa cells reduced tumor-invading bone lesions.
- We established that MAOA regulates HIF1α stability through ROS.
- The elevated levels of HIF1α result in upregulated expression of *VEGF-A*, *GLUT1* and *TWIST1* genes, resulting in an increased tumorigenesis.
- We showed that MHI-clorgyline reduced PCa cell proliferation and angiogenesis, increases apoptosis *in vitro* and *in vivo*.
- MHI-clorgyline also reduced the expression of oncogenes and cell cycle regulators that promote EMT, tumor hypoxia and cancer cell invasion and migration, indicating anti-metastatic activity of the conjugate.
- We developed *Pten/MAOA* double-knockout mouse models to study the effect of Pten and MAOA loss on the onset and progression of PCa.

5. CONCLUSION:

During the second year of the grant support, we further established the role of MAOA in human PCa progression and metastasis. Through our experimental work we defined the molecular basis of MAOA functions in PCa. Through the effort of synthetic chemistry, imaging and molecular pharmacology we developed an effective MAOA targeting strategy in tumors as well as means of inhibition of its downstream targets. Our novel MAOA inhibitor, MHI-clorgyline, is selectively delivered to PCa cells using a dye-drug conjugate platform to specifically target tumors without collateral damage to central nervous systems and the impairment of the normal tissue functions. The dye-drug conjugates can be visualized in tumors through the use of NIR imaging, which could also be utilized as a monitoring tool for the assessment of the drug efficacy, its delivery, and its impact on tumor growth and metastasis.

We found that treatment with MHI-clorgyline resulted in a reduction of cell proliferation and angiogenesis, and increase in apoptosis of PCa cells. Gene expression profiles of tumors treated with MHI-clorgyline also indicated reduction in expression of oncogenes and cell cycle regulators downstream of MAOA and increase in the levels of tumor suppressor gene *TP53* and cell cycle inhibitors. This suggests that MHI-clorgyline decreased proliferative and metastatic potential of PCa cells and tumors.

In order to further study the role of MAOA in PCa progression, we generated a *Pten/MAOA* double knockout mouse model through the deletion of *MAOA* in a conditional *Pten* knockout mouse model. These mice showed reduction in myeloid-derived suppressor cells and a delayed formation of PCa tumors, suggesting that MAOA has an immunosuppressive effect in hypoxic prostate tumors, facilitating the evasion of tumor cells from detection by the immune system.

The immediate future plans of this study are to continue *in vivo* assessment of the efficacy of our dye-drug conjugate in mouse prostate tumor xenografts and further mechanistic study of its action *in vivo*. The long-term goals are to translate our MAOA inhibitors from bench to bedside for improved treatment of PCa growth and metastasis.

6. PUBLICATIONS, ABSTRACTS, AND PRESENTATIONS:

a.

(1) Lay Press selected from over 30 news reports):

"Antidepressant May Also Fight Prostate Cancer", USC News, June 2, 2014. https://pressroom.usc.edu/antidepressant-may-also-fight-prostate-cancer/

"Enzyme used in antidepressants could help researchers develop prostate cancer treatments", HSC News, June 10, 2014.

http://hscnews.usc.edu/enzyme-used-in-antidepressants-could-help-researchers-develop-prostate-cancer-treatments/

"Antidepressants show promise for treating prostate cancer", Futurity. org , June 4, 2014.
http://www.futurity.org/antidepressants-prostate-cancer-enzyme/?utm_source=rss&utm_medium=rss&utm_campaign=antidepressants-prostate-cancer-enzyme

"Enzyme used in antidepressants could help researchers develop prostate cancer treatments", MedicalXpress, June 2, 2014.
http://medicalxpress.com/news/2014-06-enzyme-antidepressants-prostate-cancer-treatments.html

"Enzyme used in antidepressants could help researchers develop prostate cancer treatments", Science Daily, June 1, 2014.
http://www.sciencedaily.com/releases/2014/06/140601113953.htm

"Enzyme Used In Antidepressants Could Help Researchers Develop Prostate Cancer Treatments", News-Line Publishing, June 4, 2014.
http://www.newslinepublishing.com/NL_news18603_Enzyme-Used-In-Antidepressants-Could-Help-Researchers-Develop-Prostate-Cancer-Treatments

(2) Peer-Reviewed Scientific Journals: 4 Publications

Wu JB, Pan DF, Chung LWK. Near-infrared fluorescence and nuclear imaging and targeting of prostate cancer. *Transl Androl Urol* **2013**;2(3):254-264.

Wu JB, Shao C, Li X, Hu P, Chen Y-T, Li Q, Yin F, Li Y, Zhau HE, Shih JC, and Chung LWK. Monoamine oxidase A mediates prostate tumorigenesis and cancer metastasis. *J Clin Invest* **2014**, 124(7):2891-2908.

Wu JB, Shao C, Li X, Shi C, Li Q, Hu P, Chen Y-T, Dou X, Sahu D, Li W, Wang R, Zhau HE, Chung LWK. Near-infrared fluorescence imaging of cancer mediated by tumor hypoxia and HIF1α/OATPs signaling axis. *Biomaterials* **2014**, 35:8175-8185.

Wu JB, Lin T-P, Gallagher JD, Kushal S, Zhau HE, Chung LWK, Olenyuk BZ, Shih JC. Monoamine oxidase A inhibitor – near-infrared dye conjugate reduces prostate tumor growth. *J Am Chem Soc* **2014**, submitted.

Invited Articles:

Nothing to report

(3) Abstracts:

Nothing to report

b. Presentations and posters made during the last year:

Jean C. Shih:

1. National Taiwan University, Taipei, Taiwan (2014), "MAO, Cancer and Autism"
2. Taipei Medical University, Taipei, Taiwan (2014), "MAO, Cancer and Autism"
3. National Yang-Ming University, Taipei, Taiwan (2014), "MAO, Cancer and Autism"
4. China Medical University, Taichung, Taiwan (2014), "MAO, Cancer and Autism"
5. International Symposium on Water, California Institute of Technology, Pasadena, CA (2013), "MAO A, a Novel Target for Prostate Cancer Progression".

Boyang Jason Wu:

1. Cancer Biology Work-In-Progress Seminar Series, Cedars-Sinai Medical Center, Los Angeles, CA (2014), "Novel function for monoamine oxidase A in human prostate cancer"

7. INVENTIONS, PATENTS AND LICENSES: 1 Patent Application

Inventors: Shih JC, Chung LW, Zhau HE, Wu B, Olenyuk BZ
Invention Title: Monoamine Oxidase Inhibitors and Methods for Treatment and Diagnosis of Prostate Cancer
Patent Application Number: PCT/US2012/048407
Filing Date: Jul 26, 2012
Publication Number: WO2013016580 A3
Publication Date: Mar 28, 2013

8. REPORTABLE OUTCOMES:

Phase II Clinical Trial of phenelzine on non-metastatic recurrent prostate cancer. PIs: Mitch Gross, MD , Ph.D., Jean C. Shih, Ph.D

9. OTHER ACHIEVEMENTS:

Facilitated US-Taiwan International Student Exchange
Trained Ph.D. candidates in Pharmaceutical Sciences

10. REFERENCES:

1. M. Bortolato, K. Chen, J. C. Shih, Monoamine oxidase inactivation: from pathophysiology to therapeutics. *Adv Drug Deliv Rev* **60**, 1527 (Oct-Nov, 2008).
2. J. C. Shih, K. Chen, M. J. Ridd, Monoamine oxidase: from genes to behavior. *Annu Rev Neurosci* **22**, 197 (1999).
3. S. Josson *et al.*, beta2-microglobulin induces epithelial to mesenchymal transition and confers cancer lethality and bone metastasis in human cancer cells. *Cancer Res* **71**, 2600 (Apr 1).
4. S. Y. Sung *et al.*, Coevolution of prostate cancer and bone stroma in three-dimensional coculture: implications for cancer growth and metastasis. *Cancer Res* **68**, 9996 (Dec 1, 2008).
5. D. Trachootham, J. Alexandre, P. Huang, Targeting cancer cells by ROS-mediated mechanisms: a radical therapeutic approach? *Nat Rev Drug Discov* **8**, 579 (Jul, 2009).
6. V. Flamand, H. Zhao, D. M. Peehl, Targeting monoamine oxidase A in advanced prostate cancer. *J Cancer Res Clin Oncol* **136**, 1761 (Nov).
7. L. True *et al.*, A molecular correlate to the Gleason grading system for prostate adenocarcinoma. *Proc Natl Acad Sci U S A* **103**, 10991 (Jul 18, 2006).
8. L. De Colibus *et al.*, Three-dimensional structure of human monoamine oxidase A (MAO A): relation to the structures of rat MAO A and human MAO B. *Proc Natl Acad Sci U S A* **102**, 12684 (Sep 6, 2005).
9. S. Luo, E. Zhang, Y. Su, T. Cheng, C. Shi, A review of NIR dyes in cancer targeting and imaging. *Biomaterials* **32**, 7127 (2011).
10. X. Tan *et al.*, A NIR heptamethine dye with intrinsic cancer targeting, imaging and photosensitizing properties. *Biomaterials* **33**, 2230 (2012).
11. S. Luo *et al.*, A multifunctional heptamethine near-infrared dye for cancer theranosis. *Biomaterials* **34**, 2244 (2013).
12. J. B. Wu *et al.*, Near-infrared fluorescence imaging of cancer mediated by tumor hypoxia and HIF1α/OATPs signaling axis. *Biomaterials* **35**, 8175 (2014).
13. X. Yang *et al.*, Near IR heptamethine cyanine dye-mediated cancer imaging. *Clin Cancer Res* **16**, 2833 (May 15, 2010).
14. J. B. Wu *et al.*, Monoamine oxidase A mediates prostate tumorigenesis and cancer metastasis. *J Clin Invest* **124**, 2891 (Jul 1, 2014).
15. A. G. Foraker, An analysis of nuclear size and nuclear: cytoplasmic ratio in the histological diagnosis of intraepithelial carcinoma of the cervix uteri. *Cancer* **7**, 884 (Sep, 1954).

11. APPENDICES:

Copies of the published articles:

Wu JB, Shao C, Li X, Hu P, Chen Y-T, Li Q, Yin F, Li Y, Zhau HE, Shih JC, and Chung LWK. Monoamine oxidase A mediates prostate tumorigenesis and cancer metastasis. *J Clin Invest* **2014**, 124(7):2891-2908.

Wu JB, Shao C, Li X, Shi C, Li Q, Hu P, Chen Y-T, Dou X, Sahu D, Li W, Wang R, Zhau HE, Chung LWK. Near-infrared fluorescence imaging of cancer mediated by tumor hypoxia and HIF1α/OATPs signaling axis. *Biomaterials* **2014**, 35:8175-8185.

Wu JB, Pan DF, Chung LWK. Near-infrared fluorescence and nuclear imaging and targeting of prostate cancer. *Transl Androl Urol* **2013**;2(3):254-264.